Three-beam interference lithography: upgrading a Lloyd's interferometer for single-exposure hexagonal patterning

Johannes de Boor,* Nadine Geyer, Ulrich Gösele, and Volker Schmidt

Max Planck Institute of Microstructure Physics, Weinberg 2, 06120 Halle, Germany
**Corresponding author: deboor@mpi-halle.mpg.de*

Received March 17, 2009; revised April 15, 2009; accepted April 18, 2009;
posted May 6, 2009 (Doc. ID 108712); published June 3, 2009

Three-beam interference lithography is used to create hole/dot photoresist patterns with hexagonal symmetry. This is achieved by modifying a standard two-beam Lloyd's mirror interferometer into a three-beam interferometer, with the position of the mirrors chosen to guarantee 120° symmetry of exposure. Compared to commonly used three-beam setups, this brings the advantage of simplified alignment, as the position of the mirrors with respect to the substrate is fixed. Pattern periodicities from several wavelengths λ down to $2/3\lambda$ are thus easily and continuously accessible by simply rotating the three-beam interferometer. Furthermore, in contrast to standard Lloyd's interferometers, only a single exposure is needed to create hole/dot photoresist patterns. © 2009 Optical Society of America

OCIS codes: 120.3180, 120.4610, 220.3740, 220.2945, 220.4241, 260.3160.

Laser interference lithography (LIL) is a powerful technique for the fabrication of nanostructured objects and is frequently applied in scientific research [1]. Through superposition of two or more laser beams, periodic structures are created either in a photoresist [2,3] or, when high energy lasers are used, directly in the material of interest [4–6]. Applications include the fabrication of arrays of magnetic nanoparticles [7], template masks for anodized aluminum oxide [2], and silicon nanowires [8], to name but a few. A very popular setup for LIL is a two-beam Lloyd's mirror interferometer. It allows for the large-scale fabrication of nanostructures, combined with fast alignment and easily adjustable pattern sizes. Using a two-beam Lloyd's interferometer, a single exposure will create a line pattern. To obtain hole or dot arrays with square symmetry a second exposure is required, with the sample rotated by 90°. Producing hole/dot arrays with other than 90° symmetry is possible but comes at the expense of deformed hole/dot shapes. A hexagonal pattern, e.g., can be created by rotating the sample by 60° between exposures, but the obtained holes/dots will have an elliptical shape [2], which is undesirable for most applications. Thus, a two-beam Lloyd's interferometer is not an ideal setup, in particular when it comes to the fabrication of hexagonal hole/dot arrays. Hexagonal symmetry, however, is often desired, as it yields the highest possible areal density and is therefore ubiquitous in self-organized processes like anodization of aluminum [2].

Another possibility to create structures with hexagonal symmetry are three-beam setups with independently adjustable beams [9,10]. While these setups are very flexible in terms of pattern arrangement, they are generally much harder to align than a Lloyd's mirror interferometer and not as flexible in terms of periodicity.

In this Letter, we present a modified Lloyd's mirror interferometer, which allows for the fabrication of hole/dot structures with hexagonal symmetry in a single exposure. This is achieved by adding a second mirror to the interferometer in a way that the direct incident light and the reflections from the two mirrors produce an interference pattern with hexagonal symmetry. While minimizing processing steps, our three-beam setup maintains most of the usual (LIL) advantages. These are large area fabrication, ease of alignment, and flexibility in pattern size, characteristics that are achievable with standard three-beam setups only with difficulties, if at all.

Figure 1 compares the standard two-beam Lloyd's mirror interferometer (two beam) with the presented three-beam interferometer (three beam): (a)–(c) show a photograph, the wave vectors, and the resulting intensity distribution on the surface of the sample for

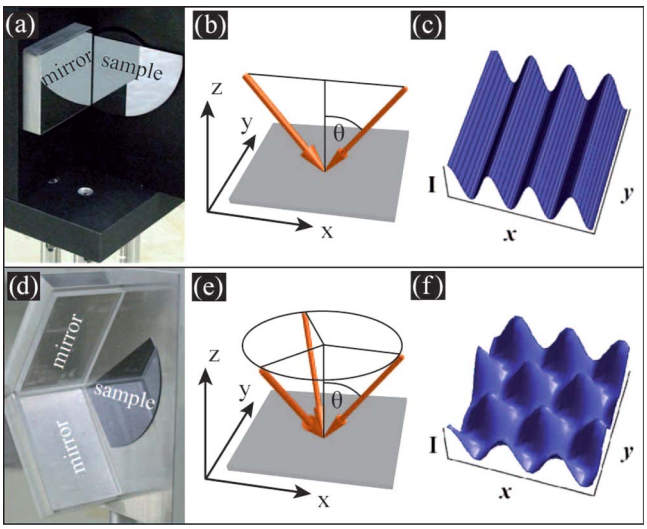

Fig. 1. (Color online) (a) Standard Lloyd's mirror interferometer, (b) incident wave vectors, and (c) corresponding line-type intensity pattern; (d) three-beam interferometer, (e) resulting wave vectors, and (f) corresponding hexagonal intensity pattern.

0146-9592/09/121783-3/$15.00

the two-beam setup, while (d)–(f) show the same for the presented three-beam setup.

In the standard setup the interference of the laser light directly incident on the sample and the laser light reflected from a mirror (perpendicular to the sample) is used to create a sinusoidal intensity distribution. The wave vectors of the direct incident light $\mathbf{k}_1$ and reflected from the mirror $\mathbf{k}_2$ are given by

$$\mathbf{k}_{1,2\text{-beam}} = k(-\sin\theta, 0, -\cos\theta),$$

$$\mathbf{k}_{2,2\text{-beam}} = k(\sin\theta, 0, -\cos\theta), \quad (1)$$

with $k = |\mathbf{k}| = 2\pi/\lambda$ in the coordinate system sketched in Fig. 1. λ denotes the wavelength of the applied laser, and θ is the angle between the incident laser beam and the normal of the sample. In the setup we present here, there are three incident waves: again the directly incident laser light plus the reflections from the two mirrors, in this case two. These mirrors are each perpendicular to the sample plane and are at an angle of 120° with respect to each other. This ensures that the wave vectors of the three waves follow a 120° degree symmetry. The wave vectors can be derived from geometrical considerations,

$$\mathbf{k}_{1,3\text{-beam}} = k(-\sin\theta, 0, -\cos\theta),$$

$$\mathbf{k}_{2,3\text{-beam}} = k(0.5\sin\theta, \sqrt{3/4}\sin\theta, -\cos\theta),$$

$$\mathbf{k}_{3,3\text{-beam}} = k(0.5\sin\theta, -\sqrt{3/4}\sin\theta, -\cos\theta). \quad (2)$$

The laser used for illumination is a frequency-doubled argon-ion laser with $\lambda = 244$ nm and a typical output power of 3 mW. The light is directed into a spatial filter consisting of focusing lens and a 10 μm diameter pinhole. The distance between the spatial filter and the sample holder is around 1 m, and typical illumination times are 1 to 5 min. The area of the exposed sample is typically >4 cm^2. Dielectric mirrors ($75\times50\times5$ mm) with a HfO_2/SiO_2 multilayer coating on a silica substrate were obtained from Laseroptik GmbH, Garbsen, Germany.

Standard silicon wafers were used as a substrate for the photoresist and were cleaned by rinsing with acetone, isopropanol, and deionized water. The photoresist (AR-N 4240, mixed with diluter AR 300-12 at ratio 1:2) was applied onto the wafer by spin coating (4000 rpm, 30 s), adhesion was improved by primer AR 300-80 (2000 rpm, 30 s). This was followed by a softbake at 85°C for 2 min, yielding a photoresist thickness of 200 nm. After exposure the sample was postbaked at 85°C for 30 min and developed in AR 300-47 for 30 s. All photochemicals were obtained from Allresist GmbH, Straussberg, Germany.

Figure 2 shows the scanning-electron-microscopy (SEM) image of the obtained photoresist pattern after an illumination time of $t = 150$ s and $\theta = 58°$. The low magnification image emphasizes the large-scale periodicity of the obtained hexagonal pattern, while the closeup shows the smooth feature of the photoresist. The distance between two adjacent intensity maxima, the periodicity p, is $p = 2\pi/|(\mathbf{k_i} - \mathbf{k_j})|$, where

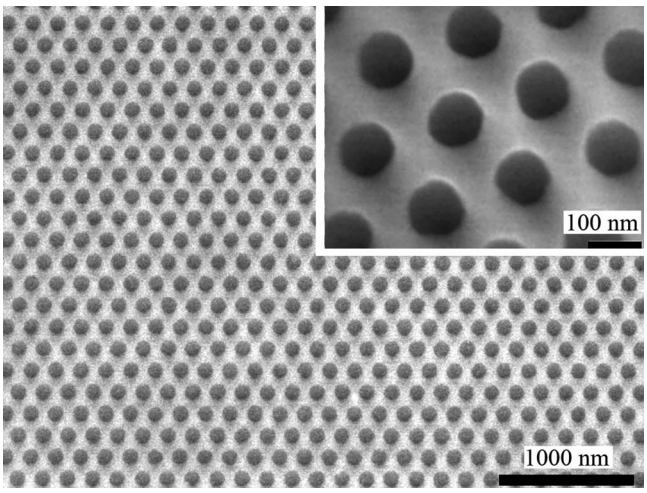

Fig. 2. SEM image of a photoresist pattern after exposure and development. The scale bar in the large, low resolution image is 1 μm and 100 nm in the inset. The periodicity is $p = 186$ nm and the holes in the photoresist have a diameter of around 100 nm.

$\mathbf{k_i}$ and $\mathbf{k_j}$ are the wave vectors of the direct incident and the reflected laser light [11], respectively. From Eqs. (1) and (2) the periodicity p in the plane of the sample can be calculated to

$$p_{2\text{-beam}} = \frac{\lambda}{2\pi\sin(\theta)}, \quad (3)$$

$$p_{3\text{-beam}} = \frac{\lambda}{1.5\pi\sin(\theta)} \quad (4)$$

for a standard Lloyd's mirror interferometer and the introduced three-beam setup, respectively. Figure 3 shows the theoretical curves for both setups plus experimental data for the three-beam setup. The ex-

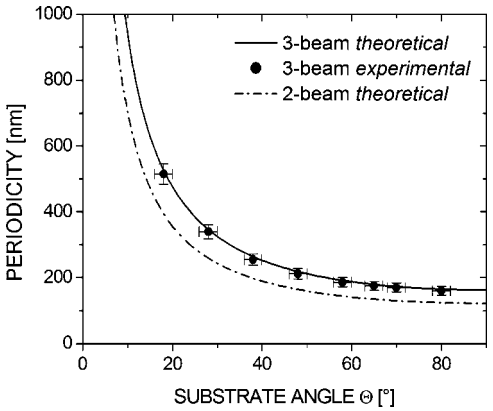

Fig. 3. Periodicity versus angle to the normal of the sample θ for a laser wavelength of $\lambda = 244$ nm. Just like for a standard Lloyd's interferometer θ is adjusted by rotating the sample holder in the plane of the optical table.The solid curve follows Eq. (4) while the markers represent experimental results, which fit the line very well. With the introduced setup periodicities from 1000 nm down to 165 nm are continuously achievable. The periodicity of a normal two-beam setup is shown as a dashed-dotted line for comparison.

perimental results agree very well with Eq. (4), and it can be seen that periodicities between 500 nm and 165 nm are continuously accessible for $\lambda = 244$ nm. The obtainable periodicities are larger by a factor of 4/3 compared to a Lloyd's mirror interferometer; however, hole/dot structures can be created with a single exposure that minimizes fabrication time and effort. Another advantage of the presented three-beam setup lies in the shape of the obtained hole/dot structures. If a pattern with hexagonal ordering is produced with a standard Lloyd's interferometer (double exposure, rotation of the sample by 60° in between) the obtained structures have an elliptical shape owing to the broken symmetry in the intensity distribution. A third exposure after a rotation of −60° would lead to arrays of round holes/dots [12], but this third exposure requires accurate alignment, which is very challenging. Figure 4 directly compares photoresist patterns obtained by (a) double exposure in the two-beam setup and (c) with patterns obtained by single exposure in the three-beam setup. Although both patterns have hexagonal symmetry, only the three-beam setup yields circular-shaped holes, whereas the standard setup creates elliptical ones. This can be quantified in terms of the ratio of major and minor axes (ellipticity) which is calculated from graphical analysis. The ellipticity is 1.54 ± 0.12 and 1.06 ± 0.04 for the samples shown in (a) and (c), respectively. Figures 4(b) and 4(d) show contour plots of the calculated intensity $I(x,y,z=0)$ for comparison. The intensities are calculated [13] using the wave vectors in Eqs. (1) and (2). The computed intensities confirm the experimental results; the intensity maxima have an elliptical shape for the two-beam interferometer, as have the resist holes, while both are round for the presented three-beam interferometer.

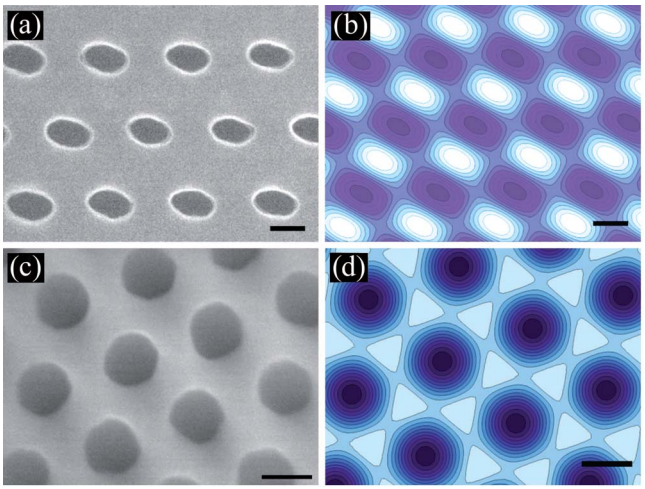

Fig. 4. (Color online) (a) SEM image of a sample fabricated in the two-beam setup, double exposure ($t = 200$ s) and a rotation of 60° in between. (b) Contour plot of the calculated intensity for this sample. (c) SEM image of a sample fabricated in the three-beam setup. (d) Calculated intensity distribution for this sample. All four images show patterns with hexagonal symmetry, but in (a) one obtains elliptical holes while in (c) they have a circular shape. The calculated intensities support this finding; the scale bar is 100 nm in each image.

LIL is a patterning technique competing with processes based on self-assembly like nanosphere lithography [14] or anodized aluminum oxide (AAO) membranes [2]. In contrast to these methods, which show only short-range order, LIL does not yield patterns with a domain substructure; stamps created with LIL can even help to improve the ordering in AAO membranes [2].

In this Letter we presented an upgraded, two-mirror version of a Lloyd's mirror interferometer. This setup allows for the fabrication of two-dimensional resist structures with a single exposure, in contrast to a standard Lloyd's interferometer. The introduced interferometer also facilitates the production of patterns with a true hexagonal symmetry. In contrast to other multiple-beam setups, this three-beam setup keeps most of the usual advantages of LIL with a Lloyd's interferometer: ease of alignment, wafer-scale fabrication of virtually defect-free photoresist patterns, and flexibility in periodicity.

We want to thank Dr. Ran Ji, Mr. Dirk Hagen, and Prof. K. Nielsch for their help with setting up the LIL. The financial support by the NANOSTRESS project is gratefully acknowledged.

References

1. S. R. J. Brueck, Proc. IEEE **93**, 1704 (2005).
2. W. Lee, R. Ji, C. Ross, U. Gösele, and K. Nielsch, Small **2**, 978 (2006).
3. R. Ji, W. Lee, R. Scholz, U. Gösele, and K. Nielsch, Adv. Mater. **18**, 2593 (2006).
4. U. Drodofsky, J. Stuhler, T. Schulze, M. Drewsen, B. Brezger, T. Pfau, and J. Mlynek, Appl. Phys. B **65**, 755 (1997).
5. A. Lasagni, D. Acevedo, C. Barbero, and F. Mücklich, Adv. Eng. Mater. **9**, 99 (2007).
6. N. Kramer, M. Niesten, and C. Schönenberger, Appl. Phys. Lett. **67**, 2989 (1995).
7. J. Martín, J. Nogués, K. Liu, J. Vicente, and I. K. Schuller, J. Magn. Magn. Mater. **256**, 449 (2003).
8. W. K. Choi, T. H. Liew, M. K. Dawood, H. I. Smith, C. V. Thompson, and M. H. Hong, Nano Lett. **8**, 3799 (2008).
9. J. Moon, J. Ford, and S. Yang, Polym. Adv. Technol. **17**, 83 (2006).
10. C. Lu, X. K. Hu, S. S. Dimov, and R. H. Lipson, Appl. Opt. **46**, 7202 (2007).
11. M. E. Walsh, Ph.D. thesis (Massachusetts Institute of Technology, 2004).
12. N. D. Lai, W. P. Liang, J. H. Lin, C. C. Hsu, and C. H. Lin, Opt. Express **13**, 9605 (2005).
13. J. L. Stay and T. K. Gaylord, Appl. Opt. **47**, 3221 (2008).
14. C. L. Haynes and R. P. V. Duyne, J. Phys. Chem. B **105**, 5599 (2001).